Orthodontics & Craniofacial Research

ORIGINAL ARTICLE

DOI: 10.1111/j.1601-6343.2010.01505.x

S Naser-ud-Din
K Thoirs
WJ Sampson

Ultrasonography, lateral cephalometry and 3D imaging of the human masseter muscle

Authors' affiliations:
S. Naser-ud-Din, Orthodontic Unit, School of Dentistry, University of Adelaide, Adelaide, SA, Australia and University of Queensland, School of Dentistry, Brisbane Queensland, Australia
K. Thoirs, School of Health Sciences, University of South Australia, Adelaide, SA, Australia
W.J. Sampson, Begg Chair, Orthodontic Unit, School of Dentistry, University of Adelaide, Adelaide, SA, Australia

Correspondence to:
Dr Shazia Naser-ud-Din
School of Dentistry
The University of Queensland
200 Turbot Street
Brisbane
Qld 4000
Australia
E-mail: s.naseruddin@uq.edu.au

Structured Abstract

Authors – Naser-ud-Din S, Thoirs K, Sampson WJ

Purpose – To develop prediction equations to assist the clinician to derive cephalometric norms from the non-invasive investigations of ultrasonography (US) and 3D imaging.

Setting and Sample Population – Adult volunteers from University of Adelaide participated in the study.

Methods – Eleven volunteers (eight women, three men; age range 22–30 years) were recruited for US and standard lateral radiographs measurements along with 3D facial imaging using a structured light technique. The three examinations were performed to assess the vertical and transverse dimensions of the face along with superficial masseter muscle dimensions. In total, 31 variables were statistically analysed for relationship among the three imaging modalities.

Results – Pearson's correlation coefficients showed highly significant correlations between lateral cephalometric (Co–Go to R3–R4) and US (volume – thickness) variables ($r = 0.92$, $p < 0.0001$; $r = 0.95$, $p < 0.0001$, respectively). Strong correlations were also observed with Co–Go and masseter muscle area derived from US $r = 0.81$ ($p = 0.01$). Similarly, strong correlations were seen between gonion–menton (Go–me) and facial width from 3D imaging ($r = 0.83$, $p = 0.003$). A high statistical significance ($p > 0.0001$) for curvilinear measurements compared with linear counterparts was revealed with the paired *t*-test. Factor analyses provided meaningful interrelationships for predictive equations generated for lateral cephalometric variables from 3D image coordinates.

Conclusions – This preliminary investigation suggests that useful clinical information for treatment planning and follow-up can be gathered without repeated exposure to ionizing radiation. For more robust predictive equations, a larger sample would be required to validate such a model.

Key words: imaging, three-dimensional; masseter muscle; predictive equations; ultrasonography

Dates:
Accepted 30 October 2010

To cite this article:
Naser-ud-Din S, Thoirs K, Sampson WJ: Ultrasonography, lateral cephalometry and 3D imaging of the human masseter muscle
Orthod Craniofac Res 2011;**14**:33–43

Introduction

Diagnostics and treatment planning in orthodontics has traditionally been based on two-dimensional representations of the face such as lateral cephalograms and photographs. Hence, the precision and ability to assess subtle changes over the course of growth or treatment, particularly in the soft tissues, have been lacking. Form and function are complexly interrelated, and no orthodontic diagnosis would be complete without a proper functional assessment (1). However, functional recordings can be time intensive and difficult to validate (2), although ultrasonography (US) and electromyography (EMG) have been used for recording muscle changes and reflexes in individuals with varying facial proportions. If comprehensive information could be gained through mathematical models which limit the number of examinations, there would be an improvement in the overall efficiency of diagnosis, treatment planning and evaluation.

Pioneering work in anthropometric facial assessment was carried out by Farkas (3) who paved the way for facial measurements with three-dimensional (3D) scanning. According to Farkas, anthropometry has an advantage over 3D imaging because of the ability to palpate bony landmarks underlying the soft tissue. However, a limitation of anthropometry is the level of cooperation of subjects required while measurements are taken, particularly in the young (4). Moreover, anthropometric measurements are confounded by the variability of soft tissues, head orientation and examiner subjectivity (4).

The physiognomy of the face is influenced by the skeletal pattern, and the transverse dimension is an important variable that can be analysed by either anthropometry or 3D techniques (5) as assessment is not available through routine lateral cephalometric analyses.

After its introduction by Thalmann-Degen in 1944 (6), 3D imaging has rapidly progressed in recent years. Primarily developed for application in industry (7, 8), imaging techniques have expanded to include stereophotogrammetry (9), 3D laser scanning, vision-based scans (Moiré tomography) in addition to the latest, safest and most cost-effective structured light 3D imaging (10).

Structured light creates a superficial, shell-like reproduction of the face enabling the digitized topology of the face to be displayed in 3D. It is considered a very safe and cost-effective way of producing a 3D image. However, like any other system, it is subject to error determined by a number of different factors; particularly, the level of background light, the level of the projected light and the distance to the subject (S. Vallance, pers. commun.). The way these factors interact can complicate the error level which is calculated by the scanning of a target containing patterns of known dimensions.

Ultrasonography is considered as a safe, non-invasive, cost-effective and comfortable diagnostic tool. Good high-resolution images of soft tissues are obtained by US, which have been claimed to be superior to magnetic resonance imaging (MRI) and computer tomography (CT) scans (11). US can be utilized in orthodontics to supplement the radiographic diagnosis of the facial pattern (11), particularly when repeated radiation dose is of concern in growing individuals. US is already utilized to monitor condylar translations in post-orthognathic surgery cases (12), to assess disc displacements (13) and to screen for juvenile idiopathic arthritis (14). Real-time US can be used to determine soft tissue function (e.g. tongue position at rest, speech and swallowing) before, during and following orthodontic or orthognathic treatment (15).

Lateral cephalometric techniques have been the mainstay for orthodontic, orthognathic and dentofacial growth studies for decades. However, this useful tool has two major limitations. First, the cumulative radiation dosage from successive films and second, the two-dimensional image is a distorted representation of the three-dimensional craniofacial region. The latter, in particular, is of significance as the complex shapes of the craniofacial region are poorly represented. Hence, the measurement and valid description of the head is limited by landmark error, reference plane and area selection. Trpkova et al. (16) in a recent meta-analysis found a limited number of landmarks with high reproducibility. Alternative methods involving mathematical models enhance the descriptive accuracy of complex shapes and increase the overall validity of the measurements (17). While there is an array of mathematical models, e.g. Euclidian distance matrix (18), thin plate spline graphical analysis, finite element morphometry (19) and Fourier analysis of cephalometric shapes (20), the major issue with these analyses is the complexity and lack of acceptance. Hence, the aim of this paper is to:

1. Elucidate a relationship between US and 3D variables with respect to the masseter muscle,
2. Confirm that curvilinear measurements are significantly different to linear and
3. Identify predictive equations that can provide alternatives to certain investigations.

Subjects and methods

Subjects

Eleven volunteers (age range 22–30 years; eight women, three men) were recruited for the current study with one male participant drop out for the 3D imaging. Approval was obtained from the Human Ethics Committees of The University of Adelaide and University of South Australia according to the Helsinki Declaration. All had a natural, healthy dentition free from dental diseases and with no overt temporomandibular disorders.

Methods

Each subject was requested to sit comfortably on a back supporting chair, in natural head posture and in a well-lit room at the same place and time with similar natural and ambient light conditions. Instructions were given to keep the eyes open if possible and to have the hair pinned back, so that the face could be imaged without any disturbance or noise.

The Mona Lisa® 3D scanner (MonaLisa® Imaging system; Tidbinbilla, Canberra, ACT, Australia) utilized a structured light projector that was placed 1.5 m away from the subject, and a horizontal light grid was flashed for 20 s with 1 s recording. Two frontal images were captured along with one left side profile image. The system used in this study comprised of a BENQ DLP projector (Dell Computers, Dallas, TX, USA; BenQ Corporation, Hsinchu, Taiwan) and Dell Inspiron laptop (Taipei, Taiwan) and two cameras (Firefly MV; Point Grey Research, Richmond, BC, Canada). Structured light was emitted in a known pattern, and images were captured with dual cameras. The 3D locations of the points in the captured image may be calculated by triangulation, which requires the relative location of the camera and projector to be known. Calibration of the light-emitting projector was used to determine the relative locations of the camera(s) by scanning a target with a checkerboard pattern of known size multiple times from different aspects. At least five different scans are used to successfully calibrate.

Each scan was captured in approximately 1 s, and the data computer processed as triangulation was performed. The raw scans produced around 200 000 3D points, which were further processed in Vr Mesh (software package for processing Point Clouds available at : http://www.vrmesh.com/) to remove unwanted scanned background data and noise. Each scan had the area of interest manually extracted from the raw scan and resampled which detected removed points to achieve a constant distance between remaining points. The resampled scans were denoised with a filter and converted into a 3D meshwork of triangles for measurement.

The images were analysed on Meshlab software (Fig. 1) (from http://meshlab.sourceforge.net/wiki/index.php/Developers linked to The Italian National Research Council's website http://www.isti.cnr.it/). Soft tissue landmarks were identified by one operator (SND). To enable best positioning, the image was magnified/rotated and points entered on soft tissue glabella (g), nasion (n), gnathion (gn), subnasale (sn) tragus (t), gonion (go), zygonion (zy), pogonion (pg) orbitale (or) and stomion (st) (3) (Fig. 1).

Nine linear measurements were calculated on each 3D image. Face height was measured from nasion to gnathion (N–Gn) while mandibular height was measured from stomion to gnathion (sto–gn) (3).

Curvilinear measurements were included to determine whether there was any significant difference with corresponding linear measurements (Fig. 2). The maxilla arc extended from tragus to subnasale and tragus (t–sn–t) and did not have an equivalent linear counterpart. The tangential mandibular depth was measured from tragus to gnathion (t–gn) from the left aspect only for consistency with US scans. A second angular measurement was generated from tragus to gonion (t–go) and gonion to gnathion (go–gn) defined as the mandibular inclination (3). This was another way to express lower vertical dimensions.

Masseter muscle images were produced at the University of South Australia using a Siemens Antares Sonoline ultrasound machine (Siemens Medical Solutions, USA Inc., Ultrasound Group, Issaquah, WA, USA). US scans were conducted in a semi-darkened room by an accredited sonographer (KT) using a 5–13 MHz linear array transducer. For consistency with previous work, light transducer pressure was applied to the region of the left masseter muscle to obtain the sonographic images (21, 22) Siescape® technology (Siemens Medical Solutions, USA Inc., Ultrasound Group) was used to produce freehand extended field of view (EFOV) image, while maintaining a transducer orientation perpendicular to the mandible. EFOV imaging allowed complete imaging of the masseter

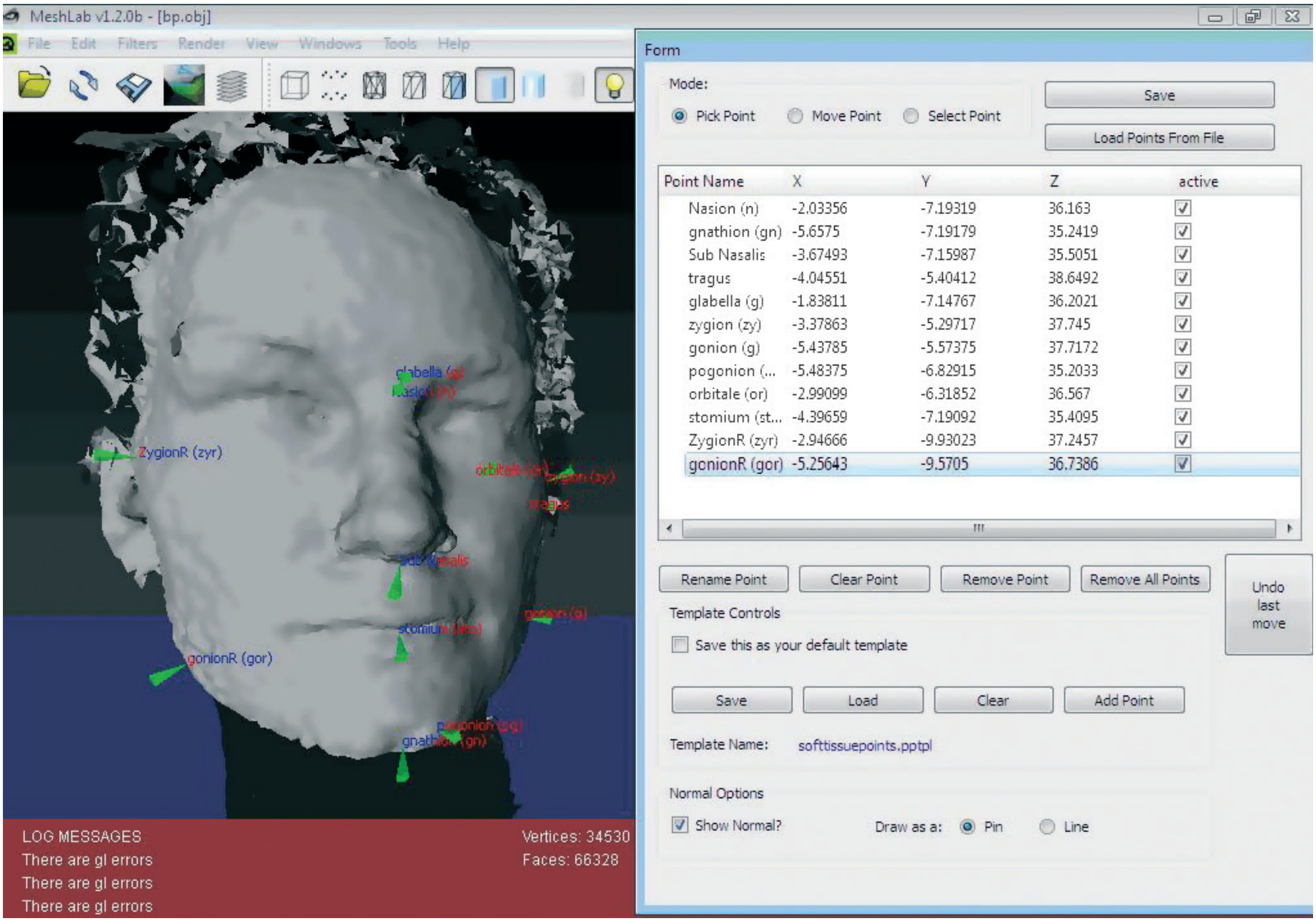

Fig. 1. Analysis of 3D scanned images using MeshLab® shows point selection for computing distances between the landmarks. Screenshot of the program.

muscle, even though the muscle was longer than the length of the ultrasound transducer.

The image plane extended between the zygomatic tubercle and gonial angle. Subjects were requested to clench in intercuspal position for 10–15 s. Measurements were taken using electronic calipers to determine length, thickness and cross-sectional area. The length of the superficial masseter muscle was measured as the distance between the zygomatic tubercule to the gonial angle. The thickness was measured as the maximum distance between the superficial and deep aspects of the masseter muscle while the cross-sectional area was traced manually on the imaged boundaries of the muscle (Fig. 3).

Each subject had a standard lateral cephalogram taken with the Siemens Nador 2 SR system (Bensheim, Germany) and a magnification factor of 1.083. The focus-film distance was 150 cm, and midsagittal plane – film distance was 11.5 cm. The exposure time was 0.64 s with 75 kV and 20 mA.

Dolphin® (Imaging & Management Solutions, Los Angles, CA, USA) and Mona Lisa® (Tidbinbilla) cephalometric analysis software systems were used to evaluate linear, angular and proportional facial skeletal variables by digitizing scanned images of the lateral cephalograms. Tracings of masseter muscle length were also performed on standard acetate paper (3M Unitek; Orthodontic Products, Monrovia, CA, USA) with a 0.3-mm graphite pencil in a darkened room. All tracings and digitization were performed by a single investigator (SND).

Linear dimensions on lateral cephalograms (Fig. 4A) were ramal length (R3–R4), articulare–gnathion (Ar–Gn) indicating mandibular length; nasion–menton (N–Me) representing the anterior face height; gonion–menton (Go–Me) representing the mandibular body length; and nasion–gnathion (N–Gn) indicating anterior vertical face height (23); R1–R2 and R3–R4 representing the ramus shape (24); and antegonial notch (AGo-Notch) which is an indicator of mandibular growth

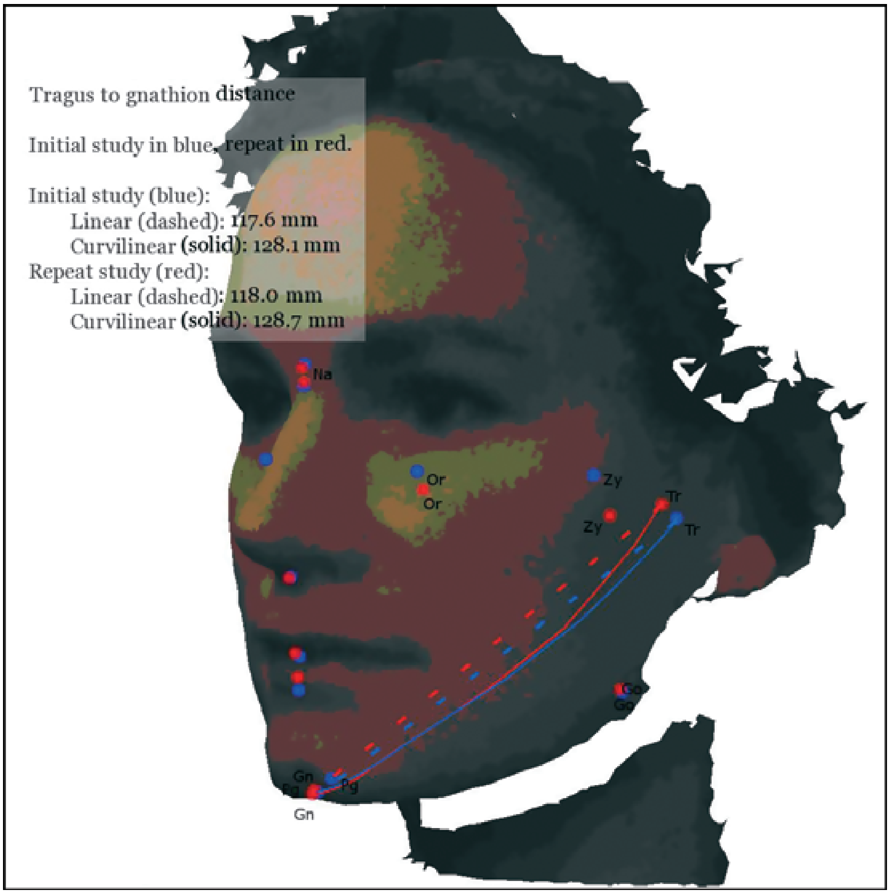

Fig. 2. Curvilinear and linear mandibular measurements for the left side of the subject. The clear advantage with 3D images as opposed to photographs. Added advantage of 3D imaging is the possibility to measure curvilinear dimensions.

rotation and also relates to the facial vertical dimension (25); masseter length from the zygomatic tubercle to gonion angle representing attachment points for the superficial masseter muscle (21, 26). The masseter lengths were measured with digital calipers.

Angular cephalometric variables in this study were gonial (go angle), upper gonial angle (UGo angle), lower gonial angle (LGo angle), overbite depth indicator (ODI) (22), maxillo–mandibular planes angle (27), and Frankfurt horizontal-mandibular plane angle (Fig. 4B,C). To determine anterior and posterior vertical proportions, the proportional vertical relationships measured were nasion–gnathion divided by articulare–gonion (N–Gn/Ar–Go); anterior lower face height (ALFH); and posterior lower face height (PLFH) (27, 28) articulare–gonion by gonion–menton (Ar–Go/Go–Me); and Jarabak ratio (N–Me/Go–Ar) (29) in Fig. 4D.

Statistics

Basic descriptive statistics with means, standard deviations and range for 3D images, US and lateral cephalometric variables were generated with the statistical package SAS 9.1 (SAS Institute, Inc., Cary, NC, USA). The data were considered normally distributed and treated accordingly. Pearson's correlation coefficients of a total of 31 variables from the three experimental settings were assessed. Factor analysis and Eigenvalues were used to assess and generate predictive equations. The confidence interval (CI) was set at 95%. Repeatability was assessed with Dahlberg's statistic and Bland and Altman method (30).

Results

Repeatability of landmarks and indices was checked with Dahlberg's statistics and the Bland and Altman method. We found significant correlations (Table 1). Descriptive statistics with mean and standard deviations for linear, proportional and angular variables taken from 3D images and lateral cephalograms were generated. Even though the sample size was relatively limited, the distribution of the data was normal.

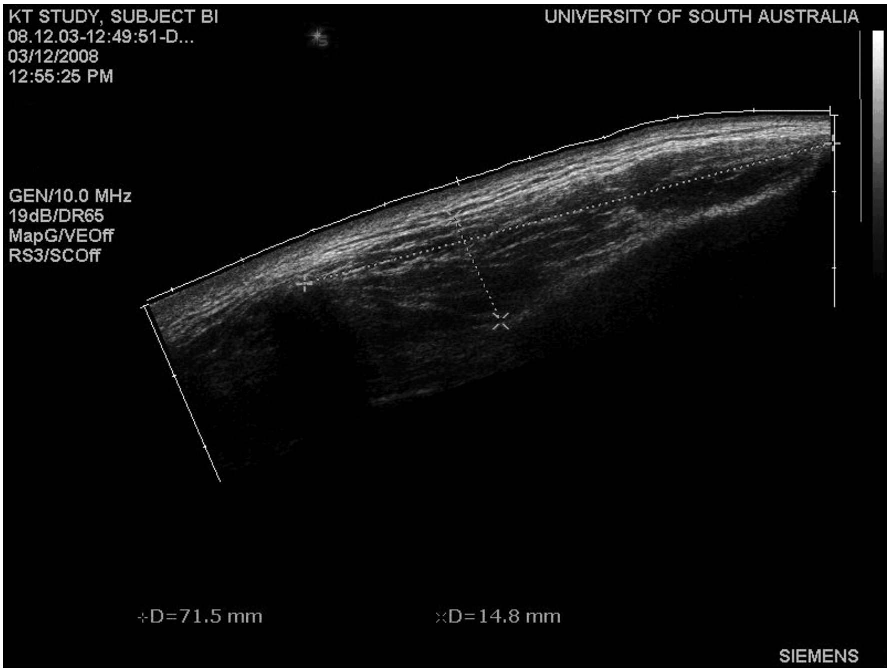

Fig. 3. US of left masseter with length and thickness along with area.

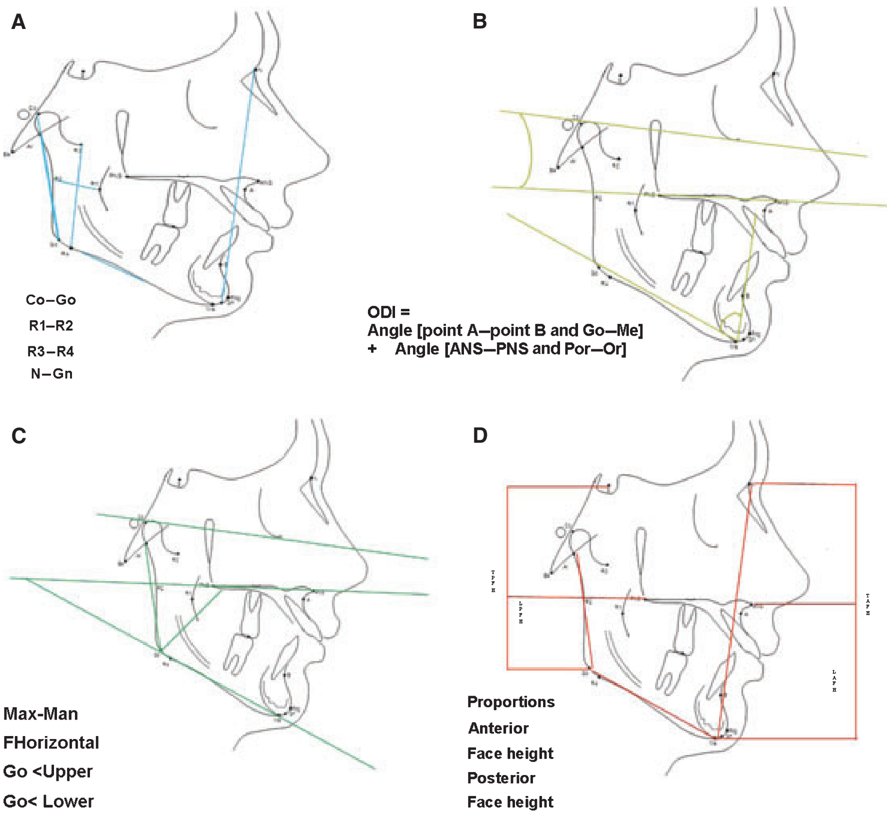

Fig. 4. Lateral cephalometric variables for linear measurements (A), overbite depth indicator (ODI) (B), angular (C) and proportional indices (D).

The highest lateral cephalograms correlations were found between Co–Go with Ricketts R3–R4 where $r = 0.92$ ($p < 0.0001$). US volume versus thickness had $r = 0.95$ ($p = 0.0001$). High correlations were found between Ar–Go from lateral cephalograms and Jaw Index from 3D imaging $r = 0.86$ ($p = 0.001$). Another very high correlation was found between Jaw Index from 3D imaging and the cephalometric variable Ar–Go ($r = 0.86$, $p = 0.001$). Tragus–gonion (t–go) (3D) was highly correlated with the cephalometric variable

***Table 1.* Method error in linear and index measurements for 3D variables**

3D variables and indices	SD	SE	Dahlberg statistic
Face width	9.54	3.01	8.86
Mandible width	4.64	1.47	0.92†
Face height	4.26	1.35	0.44‡
Mandible height	4.93	1.56	3.93
Maxilla arc	12.75	4.03	21.52
Mandibular depth linear	5.79	1.83	8.66
Mandibular depth curvilinear	6.98	2.21	12.06
Mandibular arc	13.97	4.42	24.11
Mandibular inclination	6.93	2.19	12.52
Facial index	14.95	4.73	5.52
Jaw Index	4.22	1.34	0.70†
Index jaw/facial width	13.77	4.36	9.03
Index jaw width/facial height	6.84	2.16	2.97
Index lower jaw/facial height	1.99	0.63	3.17
Index of jaw/facial height	9.75	3.08	5.11
t–go	6.31	2.10	7.90
go–gn	5.42	1.72	7.59

t, tragus; go, gonion; gn, gnathion.
†Moderately low error and ‡very low error, hence the significance of these measurements with enhanced repeatability (Dahlberg's statistics).

Co–Go at r = 0.76 ($p = 0.01$). Interestingly, face width (3D) and masseter length measured on lateral cephalograms also had a high correlation ($r = 0.78$, $p = 0.001$). Only moderate correlations were present between US and 3D images (Table 2). The ODI generally had a low and inverse correlation with US and 3D imaging variables (Table 2). However, it showed a strong correlation with lateral cephalometric variables.

Factor analysis was conducted because of the large number of variables, and Eigenvalues were produced. Two rotated factor patterns were generated for US which were then correlated to linear, angular, proportional lateral cephalometric variables. Four factors of 3D variables constituted the 3D linear, 3D proportional, 3D linear width and 3D proportional width. Curvilinear measurements were significantly different ($p > 0.0001$) from linear measurements with the paired t-test. Our findings show a significant difference ($p < 0.0001$) at 95% CI and with a standard error of 0.52 and SD = ±1.65 for the mandibular depth linear compared to mandibular depth curvilinear.

Predictive equations were developed from the multiple linear regression analyses and found significant (Table 3) on the basis of higher proportion to the variance. Only a few variables qualified for predictive equations to be significant such as tragus to gonion, mandibular arc, mandibular depth curvilinear/linear and face heights. β-weights were added into the equations as constants of each respective variable.

Discussion

Landmarks provided by anthropometry have provided a standard that may be translated into 3D imaging. However, a high level of accuracy depends upon a number of criteria. The examiner's skill and ability to identify features are of paramount importance followed by the quality and resolution of the images. This is dissimilar to real-time anthropometry where cooperation and stillness of the live subject is critical (31). Alternatively, sophistication of measuring tools and the e-tools in software could prove a valuable addition to 3D morphometry, providing a wider scope and accuracy not possible otherwise with anthropometry. For US and lateral cephalogram recording, repeatability was assessed on the entire sample and statistically assessed with Bland and Altman and Dahlberg's statistics. With regression analysis and significant correlations, predictive equations were produced to attempt to substitute for lateral cephalometric measurements. Errors in a structured light scan can manifest either as scaling error or as an absolute error. Scaling errors are best expressed as percentages, and for the MonaLisa®, mean error is 0.39% with a standard deviation of 0.31%. At larger distances, measurement scaling errors would dominate but for measurements under 150 mm, the error is better expressed as a constant with a mean of 0.53 mm and a standard deviation of 0.44 mm. Generally, the repeatability was higher with 3D laser scanning images which were of the order of 0.66% (32). More accurate scans were obtained for frontal view (33) and were chosen for the present study.

Simple methods to produce prediction equations were employed rather than resource intensive factor models such as the Bayesian or Monte Carlo factor models (34). Predictive equations are useful particularly when the investigations, such as lateral cepha-

Table 2. **Pearson's correlations coefficient showing significance between the three imaging modalities**

No of variables	LC	US	3D	Pearson's correlations r	Significance p
1	Co–Go to R3–R4			0.92	0.0001
2	Go–Me to R3–R4			0.77	0.01
3	N–Gn to ODI			−0.12	0.75
4	ODI	Volume		0.14	0.71
5		Volume – length		0.86	0.001
6		Volume – thickness		0.95	0.0001
7	R3–R4	Area		0.82	0.003
8	R3–R4	Volume		0.73	0.01
9	Go–Me	Volume		0.66	0.03
10	Co–Go	Area		0.81	0.01
11	Co–Go	Volume		0.81	0.01
12	Ar–Go	Length		0.72	0.02
13	Ar–Go	Area		0.85	0.002
14		Area	Jaw Index	0.67	0.04
15		Volume	Jaw Index	0.67	0.03
16	Go–Me		Facial width	0.83	0.003
17	Go angle upper		Face height	0.75	0.01
18	Ar–Go		Mandibular depth linear	0.67	0.04
19	Ar–Go		Mandibular depth curvilinear	0.75	0.01
20	Co–Go		t–go	0.76	0.01
21	Go angle upper		Mandibular inclination	0.70	0.02
22	Co–Go		Facial Index Facial Ht	0.64	0.05
23	Ar–Go		Jaw Index Facial Ht	0.73	0.01
24	Co–Go		Jaw Index	0.66	0.04
25	Ar–Go		Jaw Index	0.86	0.001
26	ODI		Jaw Index	−0.11	0.79

LC, lateral cephalograms; US, ultrasonography; 3D, 3D imaging; ODI, overbite depth indicator; t, tragus; go, gonion; gn, gnathion, n, nasion; Ar, articulare; me, menton; R3–R4, ramal length. Pearson correlation coefficients with p-values.

lograms, are not readily available or difficult to obtain in clinical settings. Recent work has developed predictive equations for soft tissue evaluations following orthognathic surgery (35); however, the concept of generating predictive equations from 3D images for lateral cephalometric variable estimation has been presented here for the first time. Although it can be debated that with a small sample size the value of such prediction is questionable, it does set a scene for future work.

Our Eigen values were lower than the study from Benington et al. (33) which was the first study to document masseter volume measurements with high-technology 3D US scanning. Likewise, the current study did measure the volume albeit indirectly utilizing a simple portable US unit that could find application in clinical set-ups. Similarly, when comparing with Raadsheer et al. (36), our values were slightly lower. The method error indicated that there were certain landmarks that had reduced repeatability. This may be explained by background noise and lack of clear definition in some scans. Palpation is generally advantageous in precise positioning of soft tissue gonion, but it is considered a difficult landmark overall to determine even in anthropology (3). Nasion (n) and subnasale (sn) were relatively easily identified on the 3D images. For a better view, the image was rotated upwards by 30°. This is an advantage of the scans because repositioning the

Table 3. **Predictive equations for the various variables in 3D imaging that can provide information of lateral cephalometric variables**

Predictive equation	R^2	MSE	SIG
Linear variables			
R3–R4 = 25.44932 + 0.48688*t–go	0.33	5.46	*
Masseter = −37.9501 + 0.81574*face Ht	0.88	2.19	*
N–Gn = 75.76050 + 0.20701*go–gn + 0.10290*mandibular depth linear	0.42	3.83	*
Masseter = −45.1784 + 0.67128*face Ht + 0.20006*mandible width	0.92	1.98	*
Go–Me = 58.13533 + 0.06039*mandibular arc	0.17	4.06	*
Co–Go = 28.11536 + 0.76730*t–go	0.58	5.14	*
Ar–Gn = −8.69762 + 2.50677*mandibular depth linear + −1.93239*mandibular depth curvilinear	0.67	4.16	*
Angular variables			
Go angle upper = 71.06816 + −0.36734*mandibular inclination	0.49	4.13	
Go angle = 144.2894 + −0.46133*mandibular inclination	0.47	5.33	
Proportional variables			
AFH = 52.67724 + 0.11825*Index jaw width facial height	0.01	3.06	
AFH = 52.71398 + 0.18845*Jaw Index	0.07	2.96	
AFH = 54.06144 + −0.03102*Index jaw width facial height + 0.19646*Jaw Index	0.07	3.17	

R^2, correlation; MSE, mean standard error; SIG, significance; t, tragus; go, gonion; gn, gnathion, N, nasion; Ar, articulare; Me, menton; R3–R4, ramal length; AFH, anterior face height.
Starred equations show significance at the level of $p < 0.05$. The majority of linear measurements have significant predictive equations. Grey bars are the β-weights.

live patient can be difficult and sometimes embarrassing.

Subtle soft tissue changes have been studied extensively in recent work particularly in comparing pre- and post-treatment outcomes (37–43). Similar interest in mandibular growth changes (37) and four-dimensional analyses for TMD (43) is gaining momentum in diagnostic imaging. A common criticism of new imaging techniques has been the issue of reliability which is addressed with the development of self-calibrating measuring systems (39). New directions in technology will soon be evident and need to enhance the quality of 3D images with more real-life effect. Moreover, the current software programs need substantial mouse manipulation creating undue hand and wrist fatigue where a touch screen would be ergonomically valuable. At present, lateral cephalograms still provide valuable skeletal and dental information which is vital for initial treatment planning. It is likely that these will continue to be the basis for diagnosis in the near future. Moreover, the limitations of prediction notwithstanding, a method that can assist the clinician in reducing the number of examinations would be surely welcomed by the public and orthodontic profession alike.

Clinical relevance

The trend towards non-invasive and cost-effective diagnostic procedures is on increase. Patients would welcome simple and radiation-free examinations particularly when repeated examinations are required over extended treatment times. Moreover, for evidence-based orthodontics ethically it would be viable to have repeated measures that are safe. This study endeavours towards that goal with mathematical models of predictive equations for deriving information from simple 3D examinations namely US and facial imaging.

Acknowledgements: We appreciate the funding provided by the Australian Dental Research Foundation. Thanks are due to Mrs Lucy Hatch for secretarial assistance, Dr John Fricker and Dr Scott Vallance with 3D Mona Lisa Imaging®.

References

1. Naser-Ud-Din S, Sowman PF, Dang H, Turker KS. Modulation of masseteric reflexes by simulated mastication. *J Dent Res* 2010;89:61–5.
2. Turker KS. Electromyography: some methodological problems and issues. *Phys Ther* 1993;73:698–710.
3. Farkas L. *Anthropometry of the Head and Face*, 2nd edn. New York: Raven Press Ltd; 1994.
4. Farkas LG, Tompson B, Phillips JH, Katic MJ, Cornfoot ML. Comparison of anthropometric and cephalometric measurements of the adult face. *J Craniofac Surg* 1999;10:18–25; discussion 26.
5. Nechala P, Mahoney J, Farkas LG. Maxillozygional anthropometric landmark: a new morphometric orientation point in the upper face. *Ann Plast Surg* 1998;41:402–9.
6. Ireland AJ, McNamara C, Clover MJ, House, K, Wenger, N, Barbour, ME, *et al.* 3D surface imaging in dentistry - what we are looking at. *Br Dent J* 2008;205:387–92.
7. Da Silveira AC, Daw JL Jr, Kusnoto B, Evans C, Cohen M. Craniofacial applications of three-dimensional laser surface scanning. *J Craniofac Surg* 2003;14:449–56.
8. Jeffries JM 3rd, DiBernardo B, Rauscher GE. Computer analysis of the African-American face. *Ann Plast Surg* 1995;34:318–21; discussion 21–2.
9. Quintero JC, Trosien A, Hatcher D, Kapila S. Craniofacial imaging in orthodontics: historical perspective, current status, and future developments. *Angle Orthod* 1999;69:491–506.
10. Hajeer MY, Millett DT, Ayoub AF, Siebert JP. Applications of 3D imaging in orthodontics: part II. *J Orthod* 2004;31:154–62.
11. Kubo K, Kawata T, Ogawa T, Watanabe M, Sasaki K. Outer shape changes of human masseter with contraction by ultrasound morphometry. *Arch Oral Biol* 2006;51:146–53.
12. Landes CA, Sterz M. Evaluation of condylar translation by sonography versus axiography in orthognathic surgery patients. *J Oral Maxillofac Surg* 2003;61:1410–7.
13. Emshoff R, Brandlmaier I, Bodner G, Rudisch A. Condylar erosion and disc displacement: detection with high-resolution ultrasonography. *J Oral Maxillofac Surg* 2003;61:877–81.
14. Jank S, Rudisch A, Bodner G, Brandlmaier I, Gerhard S, Emshoff R. High-resolution ultrasonography of the TMJ: helpful diagnostic approach for patients with TMJ disorders? *J Craniomaxillofac Surg* 2001;29:366–71.
15. Volk JMM, Ovsenik M. Early orthodontic treatment in children with unilateral posterior crossbite. *85th Congress of European Orthodontic Society*. Finlandia Hall, Helsinki, Finland; 2009, 16 pp.
16. Trpkova B, Major P, Prasad N, Nebbe B. Cephalometric landmarks identification and reproducibility: a meta analysis. *Am J Orthod Dentofacial Orthop* 1997;112:165–70.
17. Hurst CA, Eppley BL, Havlik RJ, Sadove AM. Surgical cephalometrics: applications and developments. *Plast Reconstr Surg* 2007;120:92e–104e.
18. Lele S, Richtsmeier JT. Euclidean distance matrix analysis: a coordinate-free approach for comparing biological shapes using landmark data. *Am J Phys Anthropol* 1991;86:415–27.
19. Sameshima GT, Melnick M. Finite element-based cephalometric analysis. *Angle Orthod* 1994;64:343–50.
20. Ferrario VF, Sforza C, Poggio CE, D'Addona A, Taroni A. Fourier analysis of cephalometric shapes. *Cleft Palate Craniofac J* 1996;33:206–12.
21. Gaudy JF, Zouaoui A, Bravetti P, Charrier JL, Guettaf A. Functional organization of the human masseter muscle. *Surg Radiol Anat* 2000;22:181–90.
22. Klocke A, Nanda RS, Kahl-Nieke B. Anterior open bite in the deciduous dentition: longitudinal follow-up and craniofacial growth considerations. *Am J Orthod Dentofacial Orthop* 2002;122:353–8.
23. Watanabe K. The relationship between dentofacial morphology and the isometric jaw-opening and closing muscle function as evaluated by electromyography. *J Oral Rehabil* 2000;27:639–45.
24. Ricketts RM, Bench RW, Hilgers JJ, Schulhof R. An overview of computerized cephalometrics. *Am J Orthod* 1972;61:1–28.
25. Satiroglu F, Arun T, Isik F. Comparative data on facial morphology and muscle thickness using ultrasonography. *Eur J Orthod* 2005;27:562–7.
26. Kasai K, Richards LC, Kanazawa E, Ozaki T, Iwasawa T. Relationship between attachment of the superficial masseter muscle and craniofacial morphology in dentate and edentulous humans. *J Dent Res* 1994;73:1142–9.
27. Benington PC, Gardener JE, Hunt NP. Masseter muscle volume measured using ultrasonography and its relationship with facial morphology. *Eur J Orthod* 1999;21:659–70.
28. Kosy E. *Reflex Control of Human Masseter Muscle by Axial Stimulation of Periodontal Mechanoreceptors During Orthodontic Tooth Movement* [Dissertation]. Adelaide: The University of Adelaide; 2003.
29. Altug Z, Iseri H, Bayazit Z, Gogen H. [Evaluation of the changes occurring in the vertical direction of the face in cases treated with activator + occipital headgear combination]. *Turk Ortodonti Derg* 1989;2:254–60.
30. Bland JM, Altman DG. Agreement between methods of measurement with multiple observations per individual. *J Biopharm Stat* 2007;17:571–82.
31. Farkas LG. Accuracy of anthropometric measurements: past, present, and future. *Cleft Palate Craniofac J* 1996;33:10–8; discussion 19–22.
32. Baik HS, Lee HJ, Lee KJ. A proposal for soft tissue landmarks for craniofacial analysis using 3-dimensional laser scan imaging. *World J Orthod* 2006;7:7–14.
33. Benington PC, Gardener JE, Hunt NP. Masseter muscle volume measured using ultrasonography and its relationship with facial morphology. *Eur J Orthod* 1999;21:659–70.
34. Petrie ABJ, Osborn J. *Further Statistics in Dentistry*. London: British Dental Association; 2002.
35. Kneafsey LC, Cunningham SJ, Petrie A, Hutton TJ. Prediction of soft-tissue changes after mandibular advancement surgery with an equation developed with multivariable regression. *Am J Orthod Dentofacial Orthop* 2008;134:657–64.
36. Raadsheer MC, van Eijden TM, van Ginkel FC, Prahl-Andersen B. Contribution of jaw muscle size and craniofacial morphology to human bite force magnitude. *J Dent Res* 1999;78:31–42.
37. Cevidanes LH, Franco AA, Gerig G, Proffit WR, Slice DE, Enlow DH et al. Assessment of mandibular growth and response to orthopedic treatment with 3-dimensional magnetic resonance images. *Am J Orthod Dentofacial Orthop* 2005;128:16–26.
38. Kau CH, Richmond S. Three-dimensional analysis of facial morphology surface changes in untreated children from 12 to 14 years of age. *Am J Orthod Dentofacial Orthop* 2008;134:751–60.
39. Kopp S, Kuhmstedt P, Notni G, Geller R. G-scan – mobile multiview 3-D measur-

ing system for the analysis of the face. *Int J Comput Dent* 2003;6:321–31.

40. Martensson B, Ryden H. The holodent system, a new technique for measurement and storage of dental casts. *Am J Orthod Dentofacial Orthop* 1992;102:113–9.
41. Papadopoulos MA, Christou PK, Athanasiou AE, Boettcher P, Zeilhofer HF, Sader R et al. Three-dimensional craniofacial reconstruction imaging. *Oral Surg Oral Med Oral Pathol Oral Radiol Endod* 2002;93:382–93.
42. Sharma AA, Lee RT. Prospective clinical trial comparing the effects of conventional Twin-block and mini-block appliances: part 2. Soft tissue changes. *Am J Orthod Dentofacial Orthop* 2005;127:473–82.
43. Terajima M, Endo M, Aoki Y, Yuuda K, Hayasaki H, Goto TK et al. Four-dimensional analysis of stomatognathic function. *Am J Orthod Dentofacial Orthop* 2008;134:276–87.